11478 *Biochemistry* **2009,** *48,* 11478–11486
DOI: 10.1021/bi9014049

BIOCHEMISTRY
including biophysical chemistry & molecular biology
Article

NMR Investigation of DNA Primer-Template Models: Guanine Templates Are Less Prone to Strand Slippage upon Misincorporation[†]

Lai Man Chi and Sik Lok Lam*

Department of Chemistry, The Chinese University of Hong Kong, Shatin, New Territories, Hong Kong

Received August 12, 2009; Revised Manuscript Received November 1, 2009

ABSTRACT: Misaligned structures can result from strand slippage during DNA replication and, if not repaired, would lead to mutations. Previously, we showed that strand slippage can occur upon misincorporation of a dNTP opposite thymine and cytosine templates, resulting in a misaligned structure with a T- or C-bulge. The formation propensity for misaligned structures was found to depend on the type of terminal base pair. In this study, we performed NMR investigations on primer-template models containing a guanine template. Our results reveal guanine templates are less prone to strand slippage than pyrimidine templates. Misalignment was found to occur only in 5′-CG templates with a downstream purine. In addition to the significance of terminal base pair and upstream nucleotide, the present study reveals the importance of the templating base and its downstream nucleotide, which also determine the propensity of strand slippage in primer-templates.

DNA replication fidelity relies on a variety of processes including selectivity of DNA polymerase, exonucleolytic proofreading function, and postreplication repair activity (*1*). High-fidelity DNA replication is crucial in order to maintain the integrity of genetic information, yet mutations are essential in facilitating translesion synthesis of otherwise replication-blocking lesions and are counterbalanced by the requirement for evolution of species (*2*). The discovery of the proofreading-deficient Y-family DNA polymerases provides new mechanistic pathways for evolution (*3*−*5*). Y-family DNA polymerases have no detectable sequence similarity with other family polymerases and lack any intrinsic exonucleolytic activity for proofreading (*6*, *7*). Their open and spacious active sites allow the accommodation of bulky adducts, wobble or Hoogsteen base pairs (*8*−*11*), and are believed to aid in continuing translesion DNA synthesis by efficiently bypassing damaged templates of bulky DNA adducts and/or replicating undamaged DNA (*5*, *12*), suggesting primer-template structures may also play a significant role in the fidelity of DNA replication. In this work, we performed NMR[1] investigations on primer-template models containing a guanine template and showed that guanine templates are less prone to strand slippage than pyrimidine templates, revealing the importance of the templating base in determining the propensity of strand slippage in primer-templates.

In recent years, crystal structures capturing undamaged misaligned DNA templates embedded in active sites of low-fidelity polymerases have been determined (*13*−*15*). It has also been demonstrated that such misaligned templates could be extended (*16*, *17*). These results support the formation and accommodation of a misaligned primer-template in the loose active site (*18*, *19*), which ultimately can lead to dislocation mutagenesis (*20*−*22*). In spite of different mechanisms proposed for strand slippage (*21*, *23*−*27*), mutation rates *in vivo* vary widely depending on the DNA sequence, its surrounding context, and orientation (*1*, *28*). Nevertheless, the sequence context effect of DNA substrate remains not well understood, especially when strand slippage occurs in unmodified DNA.

It has been suggested that misaligned intermediates may form in the absence of a polymerase, which may then be accepted for extension upon polymerase binding (*19*, *29*). In addition, since various types of DNA polymerases are likely to interact with primer-template differently, it is our primary interest to understand, from the DNA substrate point of view, how sequence context itself affects the primer-template structures. Previously, we have performed NMR structural investigations on primer-template oligonucleotide models which mimic the situation in which a dNTP has just been incorporated opposite a pyrimidine-template (*30*−*32*), revealing the significance of the terminal base pair in affecting the occurrence of misaligned primer-template structures. The template sequence upstream was also found to affect the misaligned structure upon further primer extension. Yet, whether the above findings apply to purine templates remains elusive.

In order to further our understanding of DNA sequence context effect on dislocation mutagenesis, we performed NMR investigations on primer-template models containing a guanine template in this study (Figure 1). In our previous work on pyrimidine templates, we found that misalignment was dominant (*30*−*32*). In the present study, we found that upon incorporation of dTTP, dATP, and dGTP opposite 5′-AG, 5′-TG, and 5′-CG templates, respectively, mispairing rather than misalignment was preferred in most cases. Misalignment occurred only in 5′-CG templates with a downstream purine (Figure 1d). When the nucleotide downstream was an A, both the

[†]The work described in this paper was partially supported by a grant from the Research Grants Council of the Hong Kong Special Administrative Region (Project No. CUHK401107) and a direct grant from CUHK Research Committee Funding (Project No. 2060367).

*To whom correspondence should be addressed. Phone: (852) 2609-8126. Fax: (852) 2603-5057. E-mail: lams@cuhk.edu.hk.

[1]Abbreviations: NMR, nuclear magnetic resonance; dNTP, deoxyribonucleotide triphosphate; NOE, nuclear Overhauser effect; 1D, one dimensional; 2D NOESY, two-dimensional nuclear Overhauser effect spectroscopy; NaCl, sodium chloride; NaP_i, sodium phosphate; DSS, 2,2-dimethyl-2-silapentane-5-sulfonic acid; WATERGATE, water suppression by gradient-tailored excitation.

 Published on Web 11/03/2009

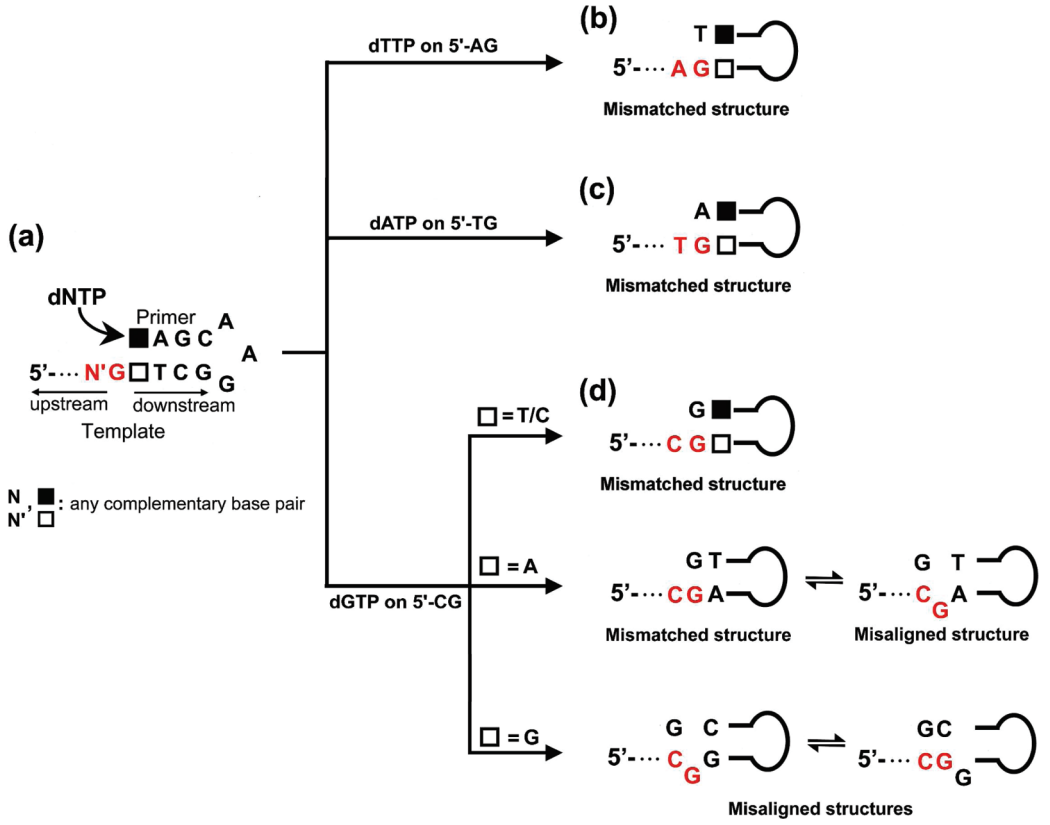

FIGURE 1: DNA primer-template models used in this study. (a) All models were designed to form a hairpin with a 5′-GAA loop. The top and bottom strands mimic the primer and template, respectively. The upstream and downstream directions are from the perspective of the template strand. For (b) 5′-AG and (c) 5′-TG templates, only mismatched conformers with terminal T·G and A·G base pairs, respectively, were observed. (d) For 5′-CG templates, mismatched conformers with a terminal G·G base pair were observed when the downstream nucleotide was a T or C. Replacing the downstream nucleotide with an A, both misaligned and mismatched conformers were observed. With a downstream G, only misaligned conformers were present, of which the G-bulge was located at either G positions in the tandem guanine template.

misaligned conformer with a G-bulge and the mismatched conformer with a terminal G·G mispair were present. When the downstream nucleotide was a G, which resulted in a tandem G template, misalignment was observed, with the G-bulge rearranging between the two consecutive guanine positions.

MATERIALS AND METHODS

Sample Design. All DNA samples were designed to form a hairpin with the top and bottom strands mimicking the primer and template, respectively (Figure 1a). The 5′-GAA hairpin loop connects the primer and template strands to simplify the sample preparative work (*33*). These samples mimic the situation in which a dNTP has just been incorporated opposite the templates. The 5′-overhang region of the samples represents the template sequence, whereas the 3′-terminal nucleotide represents the newly incorporated dNTP at the primer terminus.

Sample Preparation. All DNA samples were synthesized using an Applied Biosystems model 394 DNA synthesizer and purified using denaturing polyacrylamide gel electrophoresis and diethylaminoethyl Sephacel anion-exchange column chromatography. NMR samples were prepared by dissolving 0.5 μmol of purified DNA samples into 500 μL of buffer solution containing 150 mM NaCl, 10 mM NaP_i (pH 7.0), and 0.1 mM DSS. For the 5′-CG template with a downstream T, which shows the presence of homoduplex under the above buffer condition, it was reprepared in a buffer of 5 mM NaP_i (pH 7.0) in order to enhance the hairpin population for NMR spectral analysis.

NMR Analysis. All NMR experiments were performed using Bruker ARX-500 and AV-500 spectrometers operating at 500.13 and 500.30 MHz, respectively. For studying labile proton resonance signals, the samples were prepared in a 90% H_2O/10% D_2O buffer solution. One-dimensional imino proton spectra were acquired using the WATERGATE pulse sequence (*34*, *35*), and 2D WATERGATE-NOESY experiments were performed with a mixing time of 300 ms. For studying nonlabile proton signals, the solvent was exchanged with a 100% D_2O solution. Two-dimensional NOESY experiments were also performed with a mixing time of 300 ms, and 4K × 512 data sets were collected. For samples which showed the presence of misaligned conformer, the experiments were repeated with a mixing time of 600 ms, in order to observe the long-range NOEs. The acquired data were zero-filled to give 4K × 4K spectra with a cosine window function applied to both dimensions. In general, these experiments were conducted at 25 °C. To better observe and resolve the labile and nonlabile signals, we also repeated some of these experiments at lower temperatures.

RESULTS

In this study, we performed high-resolution NMR spectroscopic investigations focusing on 1D imino proton and 2D NOESY analyses to probe the replicating site structures of 5′-AG, 5′-TG, and 5′-CG templates after the incorporation of dTTP, dATP, and dGTP, respectively (Figure 1). Sequential proton resonance assignments were made by studying the fingerprint regions in 2D NOESY spectra (Supporting Information, S1−S16).

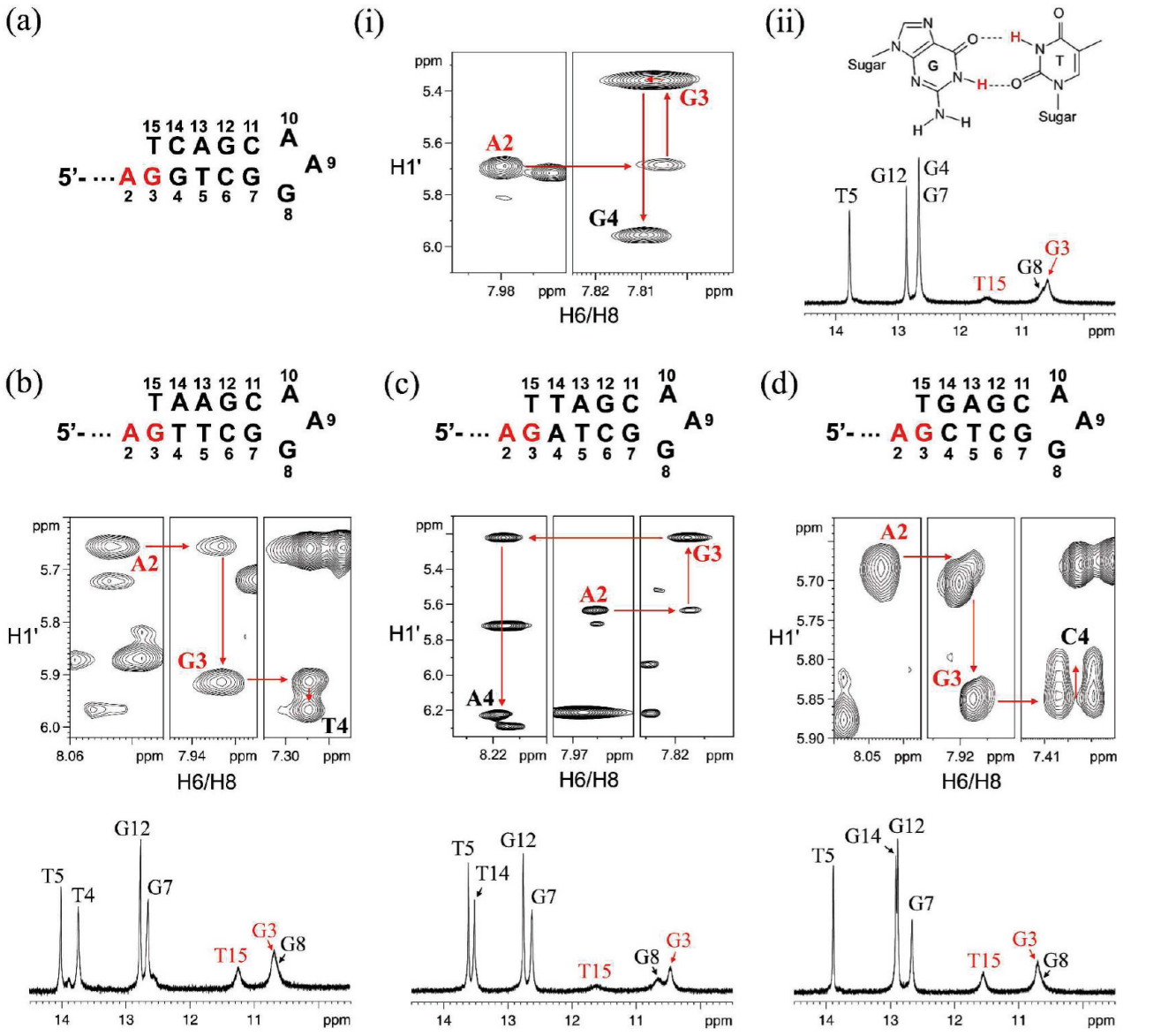

FIGURE 2: NMR evidence for mismatched conformers of 5′-AG templates. (a) Mismatched conformer was formed after incorporation of a dTTP opposite a 5′-AG template. (i) NOESY H6/H8-H1′ fingerprint region acquired at 25 °C with sample in 100% D_2O shows the sequential A2-G3 and G3-G4 NOEs. (ii) Two small imino signals corresponding to G3 and T15 iminos appeared at 5 °C. These two imino protons possibly participate in the hydrogen bonds of a proposed T·G pairing mode (*36*, *37*). The imino signal of T15 is broader and weaker than that of G3 probably due to T15 imino being more solvent exposed in the T·G mispair. The small imino signal at ~10.7 ppm corresponds to the G8 imino signal of the sheared G8·A10 mispair in the GAA loop. Similarly, the same NOESY and imino regions support the formation of mismatched conformers in 5′-AG templates upon replacing C14·G4 with (b) A14·T4, (c) T14·A4, and (d) G14·C4 base pairs.

Incorporation of a dTTP Opposite a 5′-AG Template. When dTTP was incorporated opposite a 5′-AG template, no misalignment was observed. Instead, a terminal T·G mispair was formed (Figure 1b). This was supported by the presence of sequential NOEs between A2 H1′-G3 H8 and G3 H1′-G4 H8 (Figure 2a). Moreover, two imino signals, namely, G3 and T15, were observed in the upfield imino region at 5 °C, supporting the formation of a terminal T15·G3 mispair. The imino signals at ~10.6 and 11.6 ppm were assigned to G3 and T15 imino, respectively, according to the published chemical shifts of T·G mispair, in which they possibly participate in the hydrogen bonds of a proposed T·G pairing mode (Figure 2a, ii) (*36*, *37*). Both G3 and T15 imino signals were weak and broad because of their fast exchange rates with solvent at the terminal position. The imino signal of T15 is broader and weaker than that of G3 probably due to T15 imino being more solvent exposed in the T·G mispair. No unusual A2 H1′-G4 H8 NOE and T15 imino signal that could come from a potential T15·A2 Watson−Crick base pair further support the formation of the mismatched conformer.

To investigate if the nucleotide downstream of the 5′-AG template affects the alignment of primer-template, we substituted the C14·G4 base pair with A14·T4, T14·A4, and G14·C4 base pairs, respectively. These substitutions were evidenced by the T4 (Figure 2b), T14 (Figure 2c), and G14 (Figure 2d) Watson−Crick imino signals. In all three cases, only a mismatched conformer with a terminal T·G mispair was observed, as evidenced by (i) the sequential NOEs between the second to third and third to fourth nucleotides and (ii) the presence of two upfield imino signals that correspond to the G3 and T15 imino of the terminal T15·G3 mispair. The absence of unusual NOEs between second to fourth nucleotides and T15 Watson−Crick imino signals also support the mismatched conformer.

Incorporation of a dATP Opposite a 5′-TG Template. When dATP was incorporated opposite a 5′-TG template,

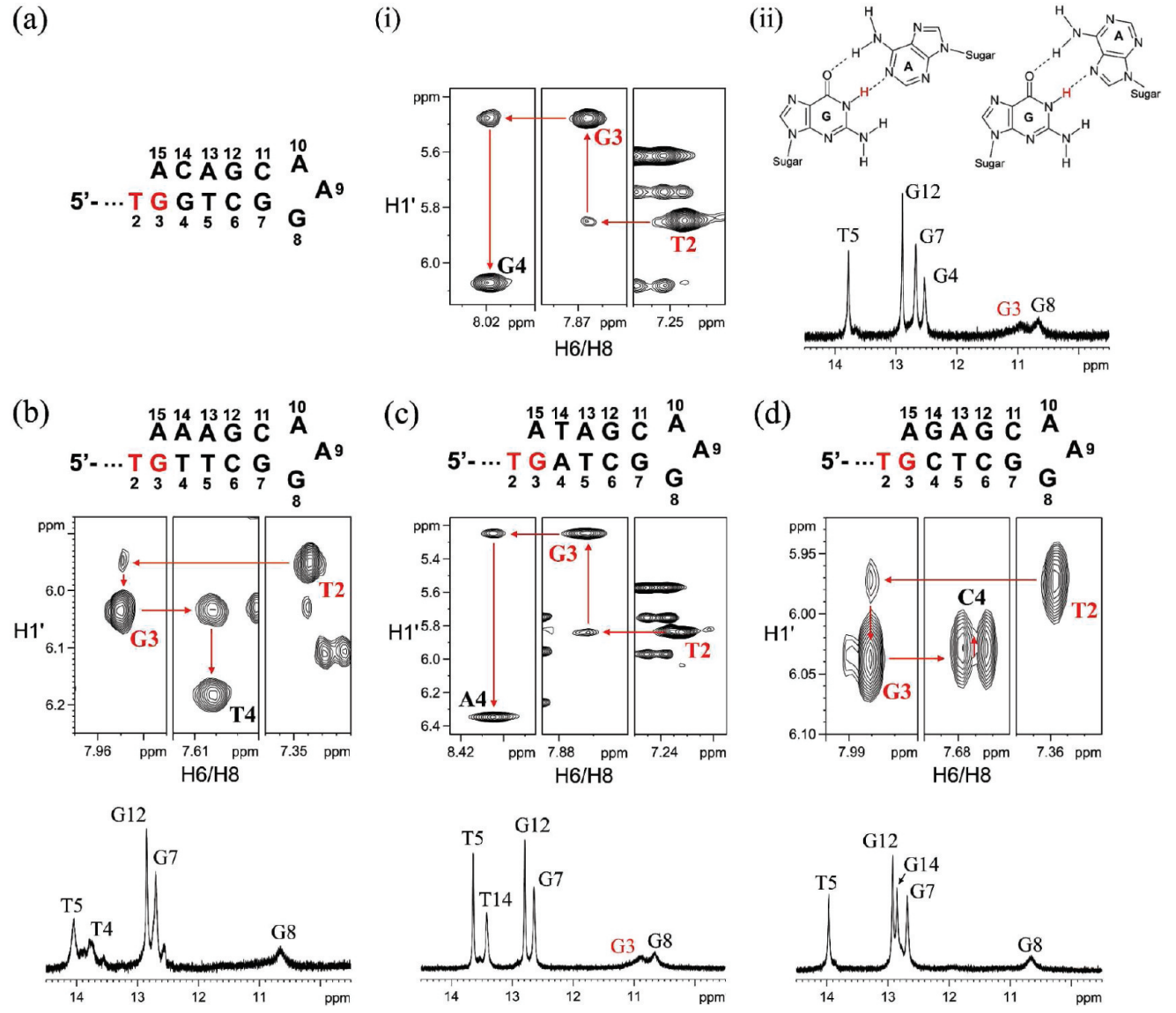

FIGURE 3: NMR evidence for mismatched conformers of 5′-TG templates. (a) Mismatched conformer was formed after incorporation of a dATP opposite a 5′-TG template. (i) NOESY H6/H8-H1′ fingerprint region acquired with sample in 100% D_2O shows the sequential T2-G3 and G3-G4 NOEs. (ii) The small imino signal at ~10.9 ppm probably comes from G3 as suggested by its involvement in the hydrogen bonds of two proposed A·G pairing modes (*38*, *39*). Similarly, the same NOESY and imino regions support the formation of mismatched conformers in 5′-TG templates upon replacing C14·G4 with (b) A14·T4, (c) T14·A4, and (d) G14·C4 base pairs. The small G3 imino was observed in (a) and (c) but not in (b) and (d) probably due to the differences in stacking interactions between the A15·G3 mispair and its flanking base pair. An overhang sequence of 5′-CAC was used in all 5′-TG samples in order to minimize homoduplex formation. For 5′-TG template with A14·T4, some imino signals from the homoduplex conformer could still be observed. The NOESY regions were acquired at 15 °C in (a) and (c) and at 25 °C in (b) and (d). All imino spectra shown in this figure were acquired at 5 °C.

a mismatched structure with a terminal A·G mispair was observed (Figure 1c). This was supported by the T2 H1′-G3 H8 and G3 H1′-G4 H8 sequential NOEs at 15 °C (Figure 3a). No unusual T2-G4 NOE nor T2 imino signal that could come from a potential A15·T2 Watson−Crick base pair was observed even at 5 °C (Figure 3a), indicating no misalignment occurred. The small imino signal at ~10.9 ppm probably comes from G3 as suggested by its involvement in the hydrogen bonds of two proposed A·G pairing modes (Figure 3a, ii) (*38*, *39*). The G3 imino signal was weak and broad because of its fast exchange with solvent at the terminal position.

Similarly, we substituted the C14·G4 base pair with A14·T4, T14·A4, and G14·C4 base pairs, respectively, in order to investigate the effect of nucleotide downstream of the 5′-TG template. Again, these substitutions were evidenced by the T4 (Figure 3b), T14 (Figure 3c), and G14 (Figure 3d) Watson−Crick imino signals. In all three cases, a mismatched conformer with a terminal A·G mispair was observed, as evidenced by the sequential NOEs between the second to third and third to fourth nucleotides. The absence of unusual NOEs between the second to fourth nucleotides and T2 Watson−Crick imino signals also supports the mismatched conformer. When the nucleotide downstream of G3 is a pyrimidine, the G3 imino was too weak to be observed (Figure 3b,d) probably due to the weaker stacking interactions between the A15·G3 mispair and its flanking base pair.

Incorporation of a dGTP Opposite a 5′-CG Template. When dGTP was incorporated opposite a 5′-CG template, three different results were observed depending on the flanking base pair downstream of the replicating site (Figure 1d). When the downstream nucleotide was a T or C, a mismatched structure with a terminal G·G mispair was observed. From the NMR

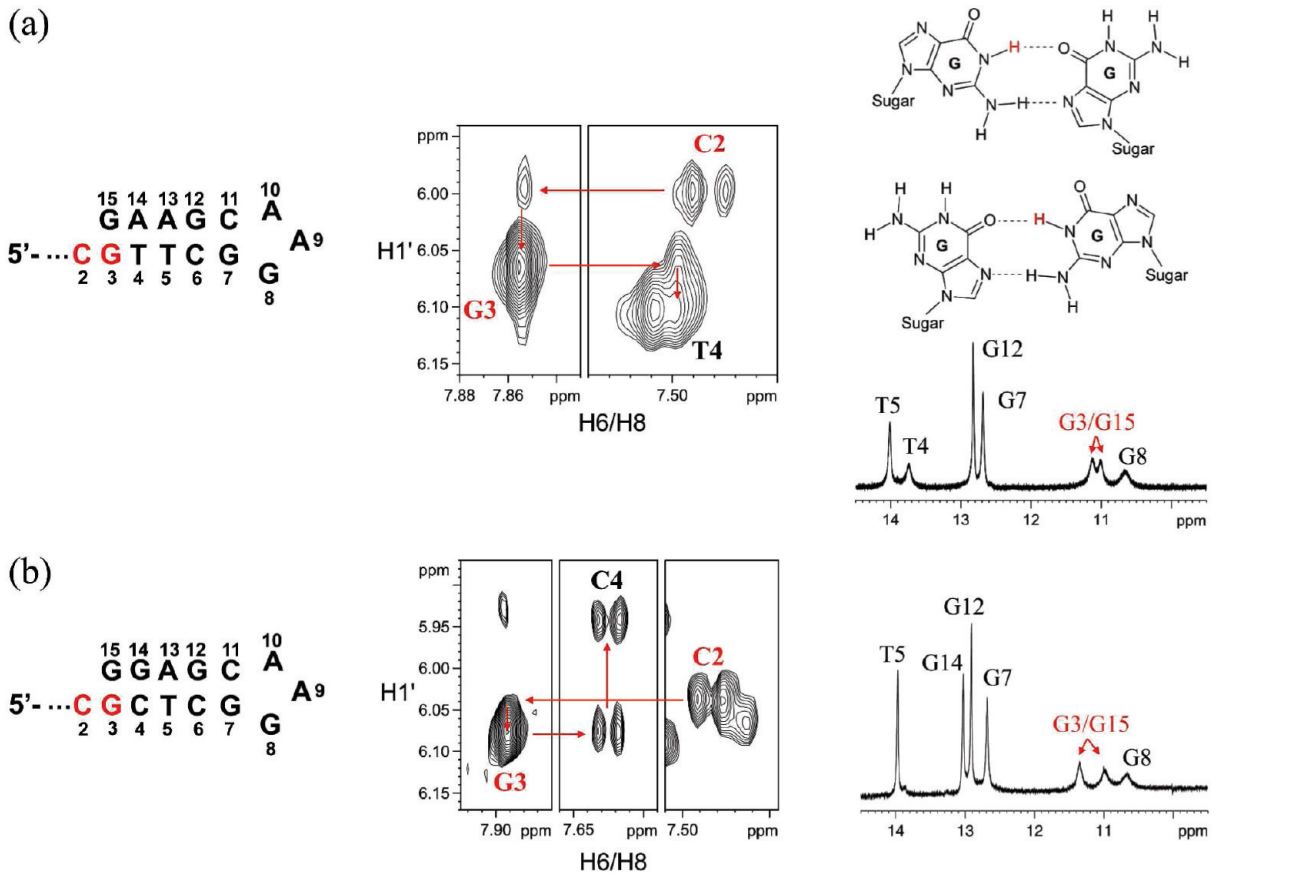

FIGURE 4: (a) The sequential C2-G3 and G3-T4 NOEs and the two G imino signals of the terminal G15·G3 mispair support the formation of the mismatched conformer in the 5′-CG template with a downstream T. G imino protons are involved in either of the two hydrogen bond G·G pairing modes (*40*, *41*), rationalizing the observation of two small G3 and G15 imino signals. Note that under normal buffer condition both hairpin and homoduplex were observed. The sample was reprepared in a buffer solution of 5 mM NaP_i (pH 7.0) for spectral analysis of the hairpin conformer. (b) With a downstream C, the sequential C2-G3 and G3-C4 NOEs and the terminal G15·G3 mispair imino signals support the mismatched conformer. Both NOESY spectra were acquired at 25 °C with samples in 100% D_2O. The imino spectra were acquired at 5 °C.

spectral results (Figure 4), the mismatched structures were supported by (i) the sequential NOEs between the second to third and third to fourth nucleotides and (ii) the presence of two imino signals that come from the terminal G15·G3 mispair. The chemical shifts of these imino protons are consistent with those of G·G mispairs in DNA duplexes, in which these protons are involved in either of the two hydrogen bond pairing modes (Figure 4a) (*40*, *41*). The G3 and G15 imino signals remain weak and broad because of their fast exchange rate with solvent due to the mispair being in the terminal position or the mispair undergoing rapid exchange between the two pairing modes. In addition, the absence of unusual NOEs between the second to fourth nucleotides and G15 Watson−Crick imino signals also supports the mismatched conformers.

When the downstream nucleotide was an A, only the intranucleotide C2 H1′-C2 H6 was observed at 25 °C. C2 was neither connected to G3 nor A4 (Supporting Information, S17). Upon lowering the temperature to 15 °C, both the sequential C2 H1′-G3 H8 and G3 H1′-A4 H8 NOEs as well as an unusual C2 H1′-A4 H8 NOE were observed (Figure 5a). The unusual NOE indicates C2 and A4 are close in space, suggesting a misaligned conformer. On the other hand, the sequential NOEs support a mismatched conformer. From the imino spectra, only a single set of imino signals was observed, suggesting the misaligned and mismatched conformers exchanged rapidly. Owing to the chemical shift of G imino in G·C Watson−Crick base pair being ~13 ppm (*42*) and that in G·G mispair being ~11 ppm (*40*), the small imino peak at ~11.6 ppm was assigned to the averaged G15 imino that comes from G15·C2 of the misaligned conformer and G15·G3 of the mismatched conformer. Similarly, the small imino signal at ~10.7 ppm was assigned to the averaged G3 imino from the two conformers.

When the primer was further extended with a C opposite the upstream G of 5′-CG template, the formation of the mismatched conformer was hampered (Figure 5b). Only the misaligned conformer with a G-bulge was observed, as evidenced by the presence of G1 and G15 imino signals (Figure 5b, i) and G1 imino-C16 amino and G15 imino-C2 amino NOEs (Figure 5b, ii), confirming the presence of G1·C16 and G15·C2 base pairs and an unpaired G3 that formed a G-bulge. Interestingly, from the NOESY spectra acquired at 25 °C, only the sequential C2-G3 and G3-A4 NOEs were observed, and no C2-A4 NOE was observed even at lower temperatures (Supporting Information, S17). Upon increasing the mixing time from 300 to 600 ms, both the sequential C2-G3 and G3-A4 NOEs as well as a C2-A4 NOE were observed (Figure 5b, iii). This presence of the long-range C2-A4 NOE at longer mixing time suggests the unpaired G remained partially stacked within the helix. The intrahelical G-bulge was also supported by the presence of base−base NOEs between C2 H6-G3 H8 and G3 H8-A4 H8 (Figure 5b, iv). The chemical shift of A4 H2 at 7.82 ppm, which is closer to the predicted value of 7.77 ppm in the case of G3 being its neighbor than 7.67 ppm in the case of C2 being its neighbor when G3 was extrahelical (*42*), also supports G3 remaining stacked between

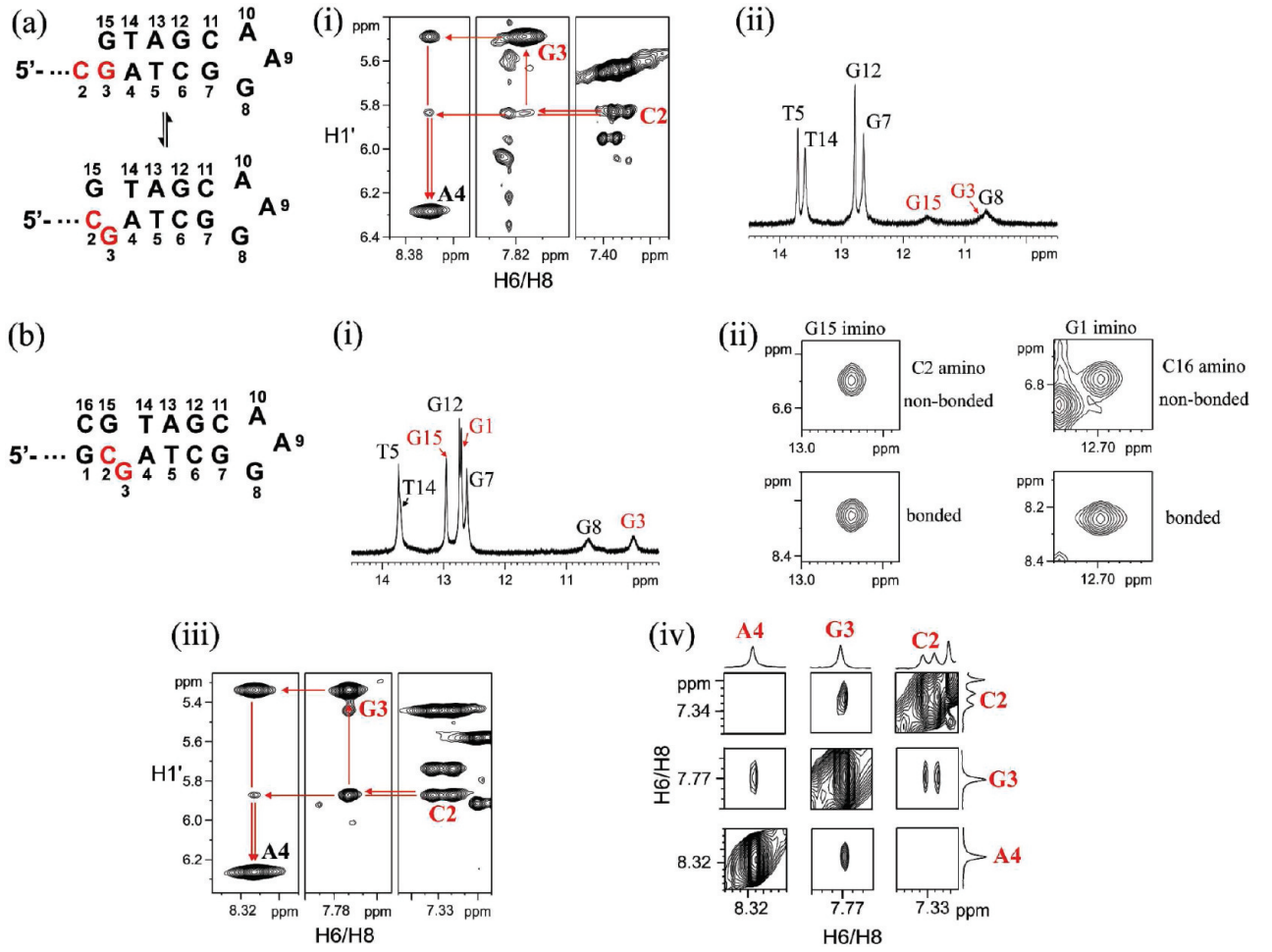

FIGURE 5: (a) For the 5′-CG template with a downstream A, both misaligned and mismatched conformers were present. At 15 °C, the unusual C2-A4 NOE supports the misaligned conformer whereas the sequential C2-G3 and G3-T4 NOEs support the mismatched conformer. Imino signals at ~11.6 and 10.7 ppm correspond to the averaged G15 and G3 of the two conformers, respectively. (b) Upon addition of a terminal C·G base pair, a further stabilized misaligned conformer containing an intrahelical G-bulge was observed. The presence of (i) G1 and G15 imino signals at 5 °C and (ii) NOEs between G15 imino-C2 amino and G1 imino-C16 amino protons at 10 °C confirm G15·C2 and G1·C16 Watson−Crick base pairs and an unpaired G3. (iii) The C2-G4 NOE was observed only at a mixing time of 600 ms at 25 °C, and (iv) the base−base NOEs between C2-G3 and G3-A4 support the G-bulge being intrahelical. The NOESY regions in (a)(i), (b)(iii), and (b)(iv) were acquired with samples in 100% D_2O.

G15·C2 and T14·A4 base pairs. Similarly, upon further primer extension with a C upstream of 5′-CG template, no realignment but a misaligned conformer with an intrahelical G-bulge was also observed (Supporting Information, S18).

When the downstream nucleotide of 5′-CG template was a G, which resulted in a tandem guanine template, a misaligned structure was observed, with a G-bulge rearranging between the consecutive guanine positions (Figure 1d). The presence of the G3-bulged conformer was supported by an unusual C2 H1′-G4 H8 NOE at 15 °C. On the other hand, a G3 H1′-T5 H6 NOE supports the G4-bulged conformer (Figure 6a, i). Although the G3-T5 NOE remained partially overlapped with the other two NOEs (C2 H5-C2 H6 and C6 H5-T5 H6) at various temperatures (Supporting Information, S19), the T5 imino signal at 13.6 ppm was much weaker and broader (Figure 6a, ii) than any T5 imino signals of the above-mentioned mismatched conformers (Figures 2−4). This suggests the neighboring G4·C14 base pair was not stable and thus supports the presence of the G4-bulged conformer. Only one set of imino peaks was observed, suggesting the G3- and G4-bulged conformers were in rapid exchange. At 5 °C, three additional small and broad imino signals were observed, with one in the Watson−Crick imino region at ~12.6 ppm and the other two at ~11.0 and ~11.8 ppm. These signals were tentatively assigned to the averaged chemical shifts of G15, G4, and G3 iminos in the two proposed misaligned conformers, respectively, according to the chemical shift prediction results of random coil and double-helical DNA (*43*).

To verify the imino proton assignments and the formation of two misaligned structures, a C·G base pair was added in order to minimize end fray and stabilize the terminal G15·C2 Watson−Crick base pair (Figure 6b). Both of the misaligned conformers were still observed, in which the G3-bulged conformer was evidenced by the C2-G4 NOE whereas the G4-bulged conformer was evidenced by the well-resolved G3-T5 NOE (Figure 6b, i). From the imino spectra, G1 and G15 imino signals were clearly observed (Figure 6b, ii), of which the imino assignments were confirmed by the NOEs between G1 imino-C16 amino and G15 imino-C2 amino that show C16·G1 and G15·C2 Watson−Crick base pairs in both conformers (Figure 6b, iii). The single set of imino peaks indicates the conformational exchange remained rapid. Compared with the T5 imino signal in Figure 5a, ii, the T5 imino signal was further weakened and broadened, suggesting that stabilizing the terminal promotes the G4-bulged conformer. Owing to the increase in population of G4-bulged conformer and thus the formation of G3·C14 Watson−Crick base pair, the averaged G3 imino signal is expected to appear more downfield.

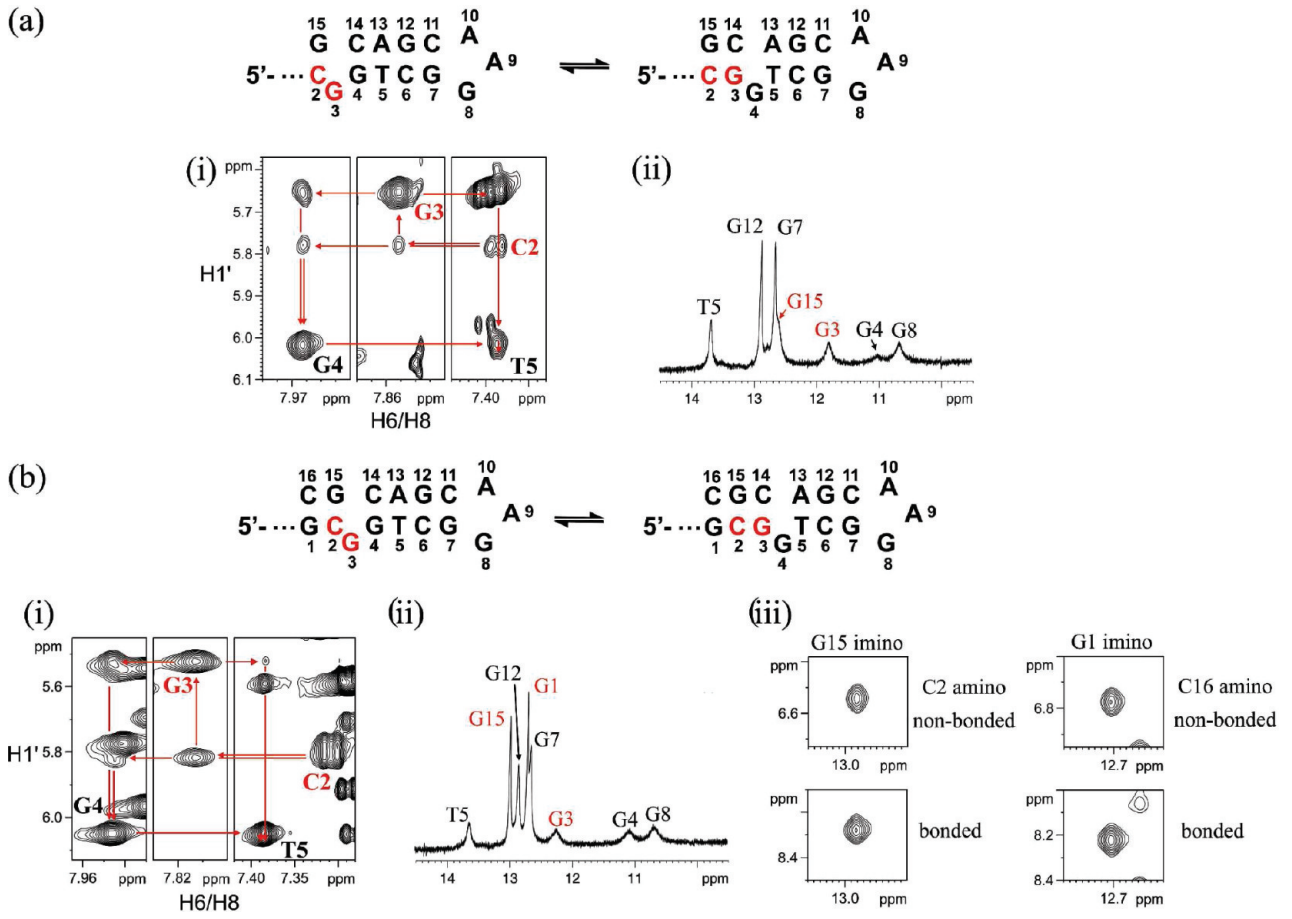

FIGURE 6: (a) For the 5′-CG template with a downstream G, misalignment was observed, with the G-bulge rearranging between the consecutive guanine positions. (i) The unusual C2-A4 and G3-T5 NOEs at 15 °C support the misaligned G3- and G4-bugled conformers, respectively. (ii) The T5 imino signal at 5 °C was weakened due to the presence of the G4-bulged conformer. (b) Upon addition of a terminal C·G base pair, the G-bulge rearrangement was still observed. (i) The C2-G4 and G3-T5 NOEs at 25 °C support the G3- and G4-bulged conformers, respectively. (ii) The G1 and G15 imino signals at 5 °C support the formation of G15·C2 and G1·C16 Watson−Crick base pairs. The T5 imino signal was further weakened, suggesting an increase in the population of the G4-bulged conformer. The tentatively assigned G3 imino signal appeared more downfield, confirming the G3 and G4 assignments. (iii) The presence of NOEs between G15 imino-C2 amino and G1 imino-C16 amino protons at 5 °C confirms G15·C2 and G1·C16 Watson−Crick base pairs. The NOESY spectra in (a)(i) and (b)(i) were acquired with samples in 100% D_2O.

These arguments are consistent with the change in chemical shift of the tentatively assigned G3 imino signal, confirming the identities of the small imino signals in Figure 5a, ii. Similar results were observed upon further primer extension with a C upstream of the 5′-CG template (Supporting Information, S20).

DISCUSSION

Strand Slippage Less Common in Guanine Templates. Our previous studies on thymine and cytosine templates showed that upon misincorporation of a dNTP that resulted in a terminal G·C or C·G base pair only misaligned conformer was observed. In case of resulting in a terminal A·T or T·A base pair, both misaligned and mismatched conformers were formed (*30*−*32*). In the present work on guanine templates, mismatched conformer was observed predominantly in regardless of the type of the resulting terminal base pair. In 5′-AG and 5′-TG templates, although they are all capable of forming a terminal A·T or T·A base pair upon misincorporation, no misaligned conformer was observed. Moreover, even for 5′-CG templates which allow the formation of a more stabilizing terminal G·C base pair, mismatched structure was also observed. This may be explained by the fact that the G·G, T·G, and A·G mismatches formed in these guanine templates are the most stable mismatches (*40*). In addition, previous studies have also shown that bulged purine was more destabilizing than bulged pyrimidine (*44*).

Misalignment Occurs Only with a Purine Downstream. In pyrimidine templates, whether the primer-template adopts a misaligned or mismatched conformer is independent of the downstream nucleotide. On the other hand, changing the downstream nucleotide of guanine templates affects the misalignment propensity. Previous study showed that bulges flanked by purines were found to be more stable than those flanked by pyrimidines (*44*). Among 5′-CG templates in this study, misalignment was observed only when the downstream nucleotide was a purine. With the downstream A, a misaligned conformer was formed but was in equilibrium with a mismatched conformer. The exchange process between these two conformers was supported by the broadenend G3 imino peak in Figure 5a when compared to that of the stabilized misaligned conformer in Figure 5b. With the downstream G, a tandem G template was resulted, allowing bulge rearrangement which is supported by the broadened G3 and G4 imino signals in Figure 6. This indicates the nucleotide downstream of the templating guanine also affects the occurrence of strand slippage, in addition to the types of terminal base pair and templating base.

G-Bulge Partially Stacked within Helix. In this work, the presence of misaligned conformers is evidenced by imino proton

signals and, more importantly, internucleotide NOEs. For misaligned conformers in pyrimidine templates, an unusual NOE between the second and fourth nucleotides (i.e., the nucleotides flanking the bulge) was observed at 25 °C at a mixing time of 300 ms (*30*−*32*). However, for the stabilized G-bulged structures (Figure 5b and Supporting Information, S18), this characteristic second to fourth NOE was observed only when the mixing time was lengthened from 300 to 600 ms, suggesting the second and fourth nucleotides were further apart. Proton chemical shift analysis and the presence of base−base NOEs between the second to third and third to fourth nucleotides (Figure 5b, iv) suggest the more bulky G-bulge, although slipped, remains partially stacked within the helix. Owing to the intrahelical G-bulge, the internucleotide H1′-H8 NOE between the 14th and 15th nucleotides was weakened when compared to that in the mismatched conformers (Supporting Information, S21). It also leads to upfield C2 H6 and H5 chemical shifts. Similar G-bulge structures were also observed in previous NMR and crystallographic studies (*13*, *44*, *45*). The unpaired G-bulge was found to be intrahelical, which can be accounted for by the fact that the stacking stabilization of the planar bicyclic ring of purine is greater than the monocyclic ring of pyrimidine (*46*). The intrahelical G-bulge may also account for the lower strand slippage propensity of guanine templates.

Homoduplex in Guanine Templates. In our previous studies on pyrimidine templates, all samples behaved as the designed primer-template structures in the buffer solution containing 150 mM NaCl and 10 mM NaP_i (pH 7.0). In this study, however, formation of homoduplex was observed in all 5′-TG templates and one 5′-CG template with a downstream T. From the imino spectra of 5′-TG templates (Supporting Information, S22), only G12 and G7 imino signals were observed and remained sharp upon lowering the temperature, revealing the terminal, penultimate, and, in some cases, the penpenultimate positions were not stable. The severely broadened thymine methyl peaks and the arising small imino signals suggest the presence of a special homoduplex conformer at lower temperatures (Supporting Information, S23). To minimize this homoduplex, we substituted the overhang 5′-ACA to 5′-CAC (Supporting Information, S24). For meaningful comparison of the results, we resynthesized all four 5′-TG templates with the 5′-CAC overhang.

For the 5′-CG template with a downstream T, the presence of hairpin and homoduplex conformers was supported by two sets of methyl and imino peaks (Supporting Information, S25a). In order to facilitate the NMR spectral analysis of the hairpin conformer, the sample was reprepared in a buffer solution containing only 5 mM NaP_i (pH 7.0) (Supporting Information, S25b). Since no obvious structural difference was observed between the hairpins formed in both buffer solutions, as evidenced by their similar chemical shifts, the structural investigation of this sample under the buffer solution containing only 5 mM NaP_i (pH 7.0) does not affect the conclusion of this work.

CONCLUSIONS

In our previous work, we found that, for pyrimidine templates, misalignment was dominant (*30*−*32*). In this work, we have demonstrated that guanine templates are less prone to strand slippage upon misincorporation. The present results suggest that, apart from the contributions of the terminal base pair, the templating base and its downstream nucleotide also affect the strand slippage propensity. To determine whether strand slippage will occur, besides the stability of the terminal base pair, other factors such as the stability of mispair in the mismatched conformer and the destabilizing effect of the bulged purine in the misaligned conformer should also be taken into account.

ACKNOWLEDGMENT

We thank R. Y. Au for preparing some of the DNA samples in this study.

SUPPORTING INFORMATION AVAILABLE

Figures showing sequential assignment, NOESY, and imino and thymine methyl proton spectra of the primer-templates. This material is available free of charge via the Internet at http://pubs.acs.org.

REFERENCES

1. Kunkel, T. A., and Bebenek, K. (2000) DNA replication fidelity. *Annu. Rev. Biochem. 69*, 497–529.
2. Tippin, B., Pham, P., and Goodman, M. F. (2004) Error-prone replication for better or worse. *Trends Microbiol. 12*, 288–295.
3. Ohmori, H., Friedberg, E. C., Fuchs, R. P., Goodman, M. F., Hanaoka, F., Hinkle, D., Kunkel, T. A., Lawrence, C. W., Livneh, Z., Nohmi, T., Prakash, L., Prakash, S., Todo, T., Walker, G. C., Wang, Z., and Woodgate, R. (2001) The Y-family of DNA polymerases. *Mol. Cell 8*, 7–8.
4. Goodman, M. F. (2002) Error-prone repair DNA polymerases in prokaryotes and eukaryotes. *Annu. Rev. Biochem. 71*, 17–50.
5. Prakash, S., Johnson, R. E., and Prakash, L. (2005) Eukaryotic translesion synthesis DNA polymerases: specificity of structure and function. *Annu. Rev. Biochem. 74*, 317–353.
6. Goodman, M. F., and Tippin, B. (2000) The expanding polymerase universe. *Nat. Rev. Mol. Cell Biol. 1*, 101–109.
7. Yang, W. (2003) Damage repair DNA polymerases Y. *Curr. Opin. Struct. Biol. 13*, 23–30.
8. Perlow-Poehnelt, R. A., Likhterov, I., Scicchitano, D. A., Geacintov, N. E., and Broyde, S. (2004) The spacious active site of a Y-family DNA polymerase facilitates promiscuous nucleotide incorporation opposite a bulky carcinogen-DNA adduct: elucidating the structure-function relationship through experimental and computational approaches. *J. Biol. Chem. 279*, 36951–36961.
9. Eoff, R. L., Irimia, A., Egli, M., and Guengerich, F. P. (2007) *Sulfolobus solfataricus* DNA polymerase Dpo4 is partially inhibited by "wobble" pairing between O6-methylguanine and cytosine, but accurate bypass is preferred. *J. Biol. Chem. 282*, 1456–1467.
10. Nair, D. T., Johnson, R. E., Prakash, L., Prakash, S., and Aggarwal, A. K. (2005) Human DNA polymerase ι incorporates dCTP opposite template G via a $G\cdot C^+$ Hoogsteen base pair. *Structure 13*, 1569–1577.
11. Yang, W. (2005) Portraits of a Y-family DNA polymerase. *FEBS Lett. 579*, 868–872.
12. Kunkel, T. A., Pavlov, Y. I., and Bebenek, K. (2003) Functions of human DNA polymerases η, κ and ι suggested by their properties, including fidelity with undamaged DNA templates. *DNA Repair (Amsterdam) 2*, 135–149.
13. Ling, H., Boudsocq, F., Woodgate, R., and Yang, W. (2001) Crystal structure of a Y-family DNA polymerase in action: a mechanism for error-prone and lesion-bypass replication. *Cell 107*, 91–102.
14. Garcia-Diaz, M., Bebenek, K., Krahn, J. M., Pedersen, L. C., and Kunkel, T. A. (2006) Structural analysis of strand misalignment during DNA synthesis by a human DNA polymerase. *Cell 124*, 331–342.
15. Wilson, R. C., and Pata, J. D. (2008) Structural insights into the generation of single-base deletions by the Y family DNA polymerase dbh. *Mol. Cell 29*, 767–779.
16. Wolfle, W. T., Washington, M. T., Prakash, L., and Prakash, S. (2003) Human DNA polymerase kappa uses template-primer misalignment as a novel means for extending mispaired termini and for generating single-base deletions. *Genes Dev. 17*, 2191–2199.
17. Cannistraro, V. J., and Taylor, J. S. (2007) Ability of polymerase η and T7 DNA polymerase to bypass bulge structures. *J. Biol. Chem. 282*, 11188–11196.
18. Kunkel, T. A., and Alexander, P. S. (1986) The base substitution fidelity of eucaryotic DNA polymerases. Mispairing frequencies, site

preferences, insertion preferences, and base substitution by dislocation. *J. Biol. Chem. 261*, 160–166.
19. Garcia-Diaz, M., and Kunkel, T. A. (2006) Mechanism of a genetic glissando: structural biology of indel mutations. *Trends Biochem. Sci. 31*, 206–214.
20. Kunkel, T. A. (1990) Misalignment-mediated DNA synthesis errors. *Biochemistry 29*, 8003–8011.
21. Kunkel, T. A., and Soni, A. (1988) Mutagenesis by transient misalignment. *J. Biol. Chem. 263*, 14784–14789.
22. Fowler, R. G., Degnen, G. E., and Cox, E. C. (1974) Mutational specificity of a conditional *Escherichia coli* mutator, mutD5. *Mol. Gen. Genet. 133*, 179–191.
23. Streisinger, G., Okada, Y., Emrich, J., Newton, J., Tsugita, A., Terzaghi, E., and Inouye, M. (1966) Frameshift mutations and the genetic code. *Cold Spring Harbor Symp. Quant. Biol. 31*, 77–84.
24. Fujii, S., Akiyama, M., Aoki, K., Sugaya, Y., Higuchi, K., Hiraoka, M., Miki, Y., Saitoh, N., Yoshiyama, K., Ihara, K., Seki, M., Ohtsubo, E., and Maki, H. (1999) DNA replication errors produced by the replicative apparatus of *Escherichia coli*. *J. Mol. Biol. 289*, 835–850.
25. Kunkel, T. A. (1986) Frameshift mutagenesis by eucaryotic DNA polymerases in vitro. *J. Biol. Chem. 261*, 13581–13587.
26. Kokoska, R. J., Bebenek, K., Boudsocq, F., Woodgate, R., and Kunkel, T. A. (2002) Low fidelity DNA synthesis by a Y family DNA polymerase due to misalignment in the active site. *J. Biol. Chem. 277*, 19633–19638.
27. Efrati, E., Tocco, G., Eritja, R., Wilson, S. H., and Goodman, M. F. (1997) Abasic translesion synthesis by DNA polymerase beta violates the "A-rule". Novel types of nucleotide incorporation by human DNA polymerase β at an abasic lesion in different sequence contexts. *J. Biol. Chem. 272*, 2559–2569.
28. Harfe, B. D., and Jinks-Robertson, S. (2000) Sequence composition and context effects on the generation and repair of frameshift intermediates in mononucleotide runs in *Saccharomyces cerevisiae*. *Genetics 156*, 571–578.
29. Bebenek, K., and Kunkel, T. A. (2000) Streisinger revisited: DNA synthesis errors mediated by substrate misalignments. *Cold Spring Harbor Symp. Quant. Biol. 65*, 81–91.
30. Chi, L. M., and Lam, S. L. (2006) NMR investigation of DNA primer-template models: structural insights into dislocation mutagenesis in DNA replication. *FEBS Lett. 580*, 6496–6500.
31. Chi, L. M., and Lam, S. L. (2007) NMR investigation of primer-template models: structural effect of sequence downstream of a thymine template on mutagenesis in DNA replication. *Biochemistry 46*, 9292–9300.
32. Chi, L. M., and Lam, S. L. (2008) Nuclear magnetic resonance investigation of primer-template models: formation of a pyrimidine bulge upon misincorporation. *Biochemistry 47*, 4469–4476.
33. Hirao, I., Kawai, G., Yoshizawa, S., Nishimura, Y., Ishido, Y., Watanabe, K., and Miura, K. (1994) Most compact hairpin-turn structure exerted by a short DNA fragment, d(GCGAAGC) in solution: an extraordinarily stable structure resistant to nucleases and heat. *Nucleic Acids Res. 22*, 576–582.
34. Piotto, M., Saudek, V., and Sklenar, V. (1992) Gradient-tailored excitation for single-quantum NMR spectroscopy of aqueous solutions. *J. Biomol. NMR 2*, 661–665.
35. Sklenar, V., Piotto, M., Leppik, R., and Saudek, V. (1993) Gradient-tailored water suppression for ^{1}H-^{15}N HSQC experiments optimized to retain full sensitivity. *J. Magn. Reson., Ser. A 102*, 241–245.
36. Patel, D. J., Kozlowski, S. A., Ikuta, S., and Itakura, K. (1984) Dynamics of DNA duplexes containing internal G·T, G·A, A·C, and T·C pairs: hydrogen exchange at and adjacent to mismatch sites. *Fed. Proc. 43*, 2663–2670.
37. Hare, D., Shapiro, L., and Patel, D. J. (1986) Wobble dG X dT pairing in right-handed DNA: solution conformation of the d(C-G-T-G-A-A-T-T-C-G-C-G) duplex deduced from distance geometry analysis of nuclear Overhauser effect spectra. *Biochemistry 25*, 7445–7456.
38. Patel, D. J., Kozlowski, S. A., Ikuta, S., and Itakura, K. (1984) Deoxyguanosine-deoxyadenosine pairing in the d(C-G-A-G-A-A-T-T-C-G-C-G) duplex: conformation and dynamics at and adjacent to the dG X dA mismatch site. *Biochemistry 23*, 3207–3217.
39. Webster, G. D., Sanderson, M. R., Skelly, J. V., Neidle, S., Swann, P. F., Li, B. F., and Tickle, I. J. (1990) Crystal structure and sequence-dependent conformation of the A·G mispaired oligonucleotide d(CGCAAGCTGGCG). *Proc. Natl. Acad. Sci. U.S.A. 87*, 6693–6697.
40. Peyret, N., Seneviratne, P. A., Allawi, H. T., and SantaLucia, J., Jr. (1999) Nearest-neighbor thermodynamics and NMR of DNA sequences with internal A·A, C·C, G·G, and T·T mismatches. *Biochemistry 38*, 3468–3477.
41. Lane, A. N., and Peck, B. (1995) Conformational flexibility in DNA duplexes containing single G·G mismatches. *Eur. J. Biochem. 230*, 1073–1087.
42. Altona, C., Faber, D. H., and Westra Hoekzema, A. J. A. (2000) Double-helical DNA ^{1}H chemical shifts: an accurate and balanced predictive empirical scheme. *Magn. Reson. Chem. 38*, 95–107.
43. Lam, S. L. (2007) DSHIFT—a web server for predicting DNA chemical shifts. *Nucleic Acids Res. 35*, W713–717.
44. LeBlanc, D. A., and Morden, K. M. (1991) Thermodynamic characterization of deoxyribooligonucleotide duplexes containing bulges. *Biochemistry 30*, 4042–4047.
45. Woodson, S. A., and Crothers, D. M. (1988) Structural model for an oligonucleotide containing a bulged guanosine by NMR and energy minimization. *Biochemistry 27*, 3130–3141.
46. Bommarito, S., Peyret, N., and SantaLucia, J., Jr. (2000) Thermodynamic parameters for DNA sequences with dangling ends. *Nucleic Acids Res. 28*, 1929–1934.